Bioorganic Chemistry 81 (2018) 184–190

Contents lists available at ScienceDirect

Bioorganic Chemistry

journal homepage: www.elsevier.com/locate/bioorg

Design, synthesis, crystal structures and anticancer activity of 4-substituted quinolines to target PDK1

K.N. Vennila[a], D. Sunny[b], S. Madhuri[b], Samuele Ciattini[c], Laura Chelazzi[c], Kuppanagounder P. Elango[a,*]

[a] Department of Chemistry, Gandhigram Rural Institute (Deemed to be University), Gandhigram 624 302, India
[b] National Institute of Animal Biotechnology, Hyderabad 500 049, India
[c] Structural Crystallography Center, University of Florence, Sesto Fiorentino (Florence), Italy

ARTICLE INFO

Keywords:
PDK1
Quinoline
Induced fit docking, A549 inhibitor

ABSTRACT

The induced fit docking of anilino quinoline scaffold results in the required hydrogen bonding interactions with amino acid residues in the orthosteric site of 3 Phosphoinositide dependent kinase (PDK1). The rational design of 4-substituted amino quinolines is carried out and eight compounds are synthesized. Four crystal structures are determined and their binding mode with adenosine triphosphate (ATP) site of PDK1 is analyzed. The anticancer activity in A549 cell lines of the test compounds by MTT assay resulted in an inhibitor with IC_{50} value of 0.96 μM which is less than the pemetrexed, a marketed lung cancer drug.

1. Introduction

Protein kinases are rich source of targets for the development of chemical probes and therapeutics, as the dysregulation of protein phosphorylation mediated by them leads to progression of various cancers [1]. Among number of kinase targets identified in different cancers, PDK1 is recently found to be an attractive one as it downstreams the activation of 24 different kinases in the cell signaling pathway and is the key regulator for cell migration and cell dissemination [2]. It was also reported that the most aggressive types such as acute myeloid leukemia, melanoma and esophageal squamous cell carcinoma, lung cancer affected cells are rich in PDK1 expression. Also, evidence is being accumulated suggesting that PDK1 is overexpressed in majority of human breast cancer cell lines [3–7]. Thus different PDK1 inhibition strategies and medicinal chemistry efforts are continuously reported in order to come out with a highly potent therapeutic drug.

In view of its three dimensional structure, PDK1 has an ATP binding site (orthosteric) and PIF pocket binding site (allosteric). The inhibition of intrinsic kinase activity is appropriate where the corresponding pathways are kinase dependent such as AKT phosphorylation inhibition. Tamgüney et al. [8] have demonstrated that the PDK1 inhibition barely affects cell growth under regular culture conditions and it sensitizes cells to apoptotic stimuli. It is also suggested that, targeting PDK1 by itself or in combination with standard chemotherapeutics could be a beneficial treatment for cancer. Many orthosteric inhibitors for PDK1 are developed in which most of them are ATP competitive inhibitors such as azaindoles [9], aminoindazoles [10], imidazo quinolones [11], dibenzo naphthrydines [12,13], oxindoles [14], pyrrolo pyrimidines [15] etc. Recent results proved that the mechanism of action of few ATP binding site inhibitors with allosteric behavior (affecting the distant site specifically) such as PS653 [16] produced conformational changes in the protein secondary structures. PS653 shown in Fig. 1 favors an open-hinge conformation and breaks the allosteric communication by stabilizing the αB and αC helices lining the PIF pocket. Together with few allosteric inhibitors, it is still continuing to develop the substrate selective ATP site inhibitors for PDK1. At the same time, Rettenmeir et al. [17] determined the complete suppression of PDK1 signaling by dual targeting approach. It is inferred that the interference of PIF pocket ligands in recruiting substrates lowers threshold of active site occupancy for ATP site binders. It is interesting to know that up to date, though numerous inhibitors are reported for PDK1 in many patents and papers, only one (GSK2334470) shown as (I) in Fig. 1 is approved by FDA and this may be due to many factors such as selectivity, solubility, non-optimal safety profiles, weak inhibition and lack of efficacy. Therefore there exists always a need for potent, selective ATP site inhibitors for PDK1.

A derivative of 3-Amino-quinolin-2(1H)-one scaffold was identified to have an appropriate geometry and electronic properties for the ATP binding site. In spite of varying the substituents in **II**, the inhibition was found to be very weak towards PDK1 [15,18]. Quinoline derivatives are

* Corresponding author.
E-mail address: drkpelango@rediffmail.com (K.P. Elango).

https://doi.org/10.1016/j.bioorg.2018.08.007
Received 13 June 2018; Received in revised form 31 July 2018; Accepted 6 August 2018
Available online 07 August 2018
0045-2068/

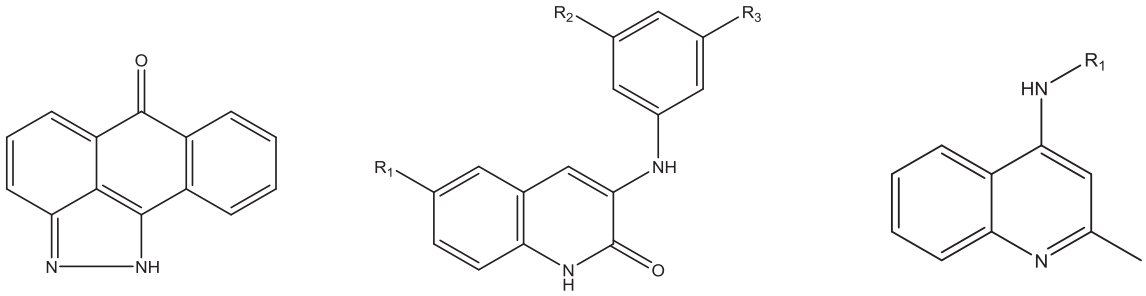

Fig. 1. PS653 (I), 3-Anilino-quinolin-2(1H) analogs (II) and Aminoquinoline analogs (III).

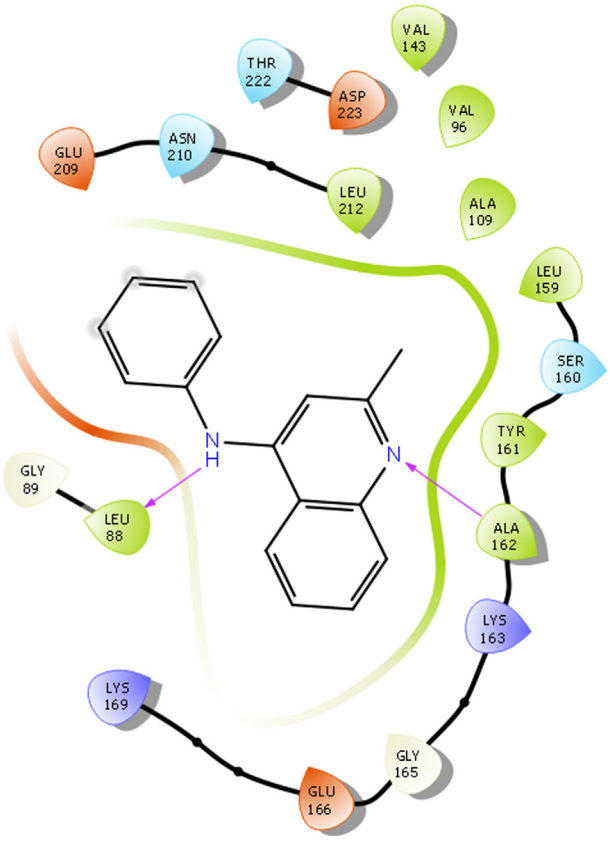

Fig. 2. Interaction of anilino quinoline with PDK1 at the ATP site.

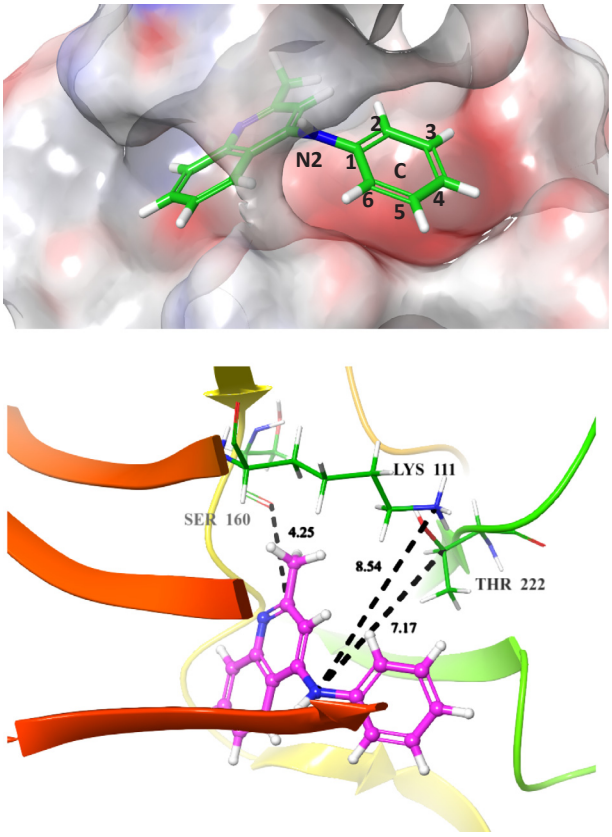

Fig. 3. (a) Anilinoquinoline scaffold in the ATP site of PDK1 (b) Distance between Lys111 and Thr222 from anilinoquinoline (c) Aminosubstituents with compatible distance to interact with Lys111 and Thr222.

potentially bioactive and no quinoline substituted potent inhibitors for PDK1 were reported so far.

Considering the shape and structural similarities of **I** and **II**, an attempt was made to analyze the binding mode of 4-anilino quinoline scaffold with PDK1 by induced fit docking protocol. The blind docking of the scaffold with grid covering the whole protein confirmed the preference of anilino quinoline to ATP binding site rather than the PIF pocket.

To our expectation, two hydrogen bonds were observed. The nitrogen atom at position-1 of the quinoline core formed hydrogen bond with the backbone of Ala162 and the other aromatic nitrogen atom with Leu88 of PDK1 in the active site. It is inferred from the ligand interaction diagram (Fig. 2) that the substitutions at 3rd position of the phenyl ring which is in the solvent exposure region will lead to a better binder by forming hydrogen bonds with other important residues like Thr222 and Lys111 in the active site. From the docking results and by visualizing the interactions with the active site, the substitutions at R_1 of III (Fig. 1) and the replacement of methyl group in quinoline ring with suitable pharmacophoric feature may lend support to better binding with key amino acid residues Ser160, Thr222 and Lys111. Also, by extending the amine substituent region, it is expected that the ligand binding part will move close to Thr222, Lys111 and Asp223 and possibly make interactions. Considering the afore mentioned, herein we have reported the synthesis and characterization of a series of eight quinoline derivatives as PDK1 inhibiting agents. The contribution of different heterocycles and fluorine substituents was anticipated and the influence of position of phenyl moiety on their antiproliferative activities was investigated. Finally, the study of cell proliferation in lung adenocarcinoma (A549), *in vitro* prediction and analysis of PDK-1 and ligand complexes were carried out.

2. Materials and methods

2.1. Computational methods

The properties such as log P, *n*-octanol/water partition coefficients, drug likeliness for kinase and ADMET/TOX were calculated by ChemAxon algorithm available in Marvinview18.1 and Qikprop in

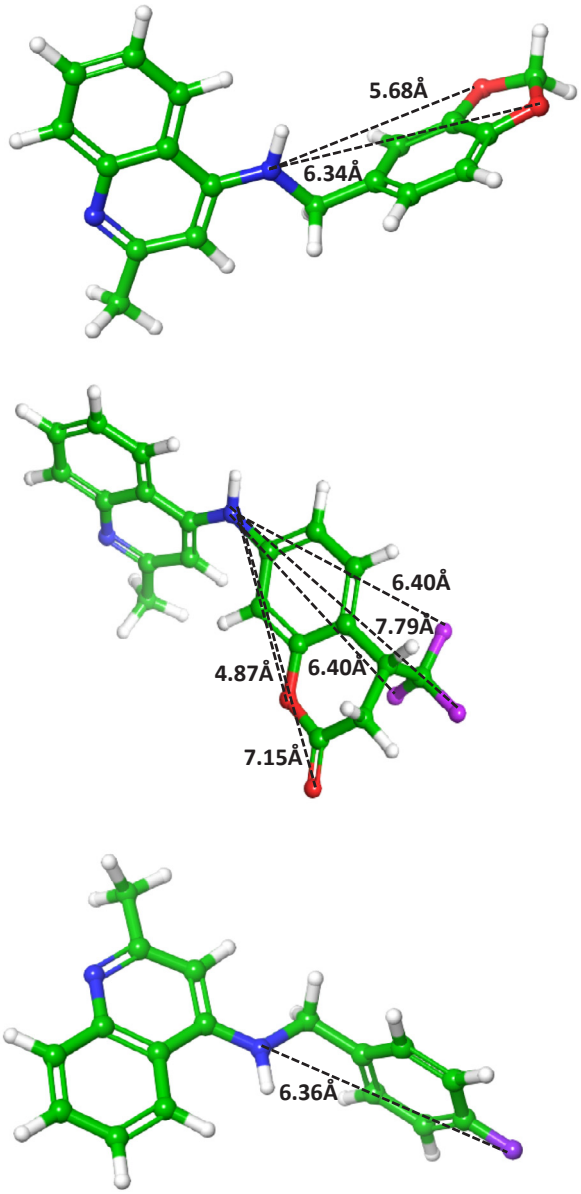

Fig. 3. (*continued*)

Schrodinger suite[16]. Structures of the compounds (**1a-c,e)** were sketched in using build panel and were prepared for docking using Ligprep module [19] implemented in Maestro 11 [31] (Schrodinger LLC). The molecules were subjected to energy minimization with OPLS-2005 force field [20] to generate single low energy 3-D structure for each input structure. The three dimensional structural coordinates of compounds **1d**, **1f-h** determined from single crystal X-ray diffraction were used as such for ligand docking. The crystallographic structure of human PDK-1 in complex with ATP (protein data bank PDB ID: 4RRV at 1.41 Å resolution) was used for all the docking simulations performed. Protein was prepared by removal of solvent molecules coupled with the addition of hydrogen atoms using Prepwizard in Maestro. The missing side chains were built using prime and the active site was visually inspected and the appropriate corrections were made for tautomeric states of histidine residues, orientations of hydroxyl groups, and protonation states of basic and acidic residues. The hydrogen atoms were minimized using OPLS2005 force field, while constraining all the heavy atoms (non-hydrogen) to their original positions. The protein with optimized hydrogen coordinates was finally saved as a separate file to be used for docking. For all the molecules, Induced Fit Docking (IFD) protocol implemented in Glide [20] was used to carry-out the docking simulation.

2.2. Chemicals

All the chemicals such as 4-chloroquinaldine, various amines (2,3-dihydrobenzo [b][1,4]dioxin-6-amine, benzo[d][1,3]dioxol-5-yl-methanamine, 3,4-dimethoxy aniline, benzo[d][1,3]dioxol-5-amine, 7-amino-4-(trifluoromethyl)-2H-chromen-2-one, 2-(pyridin-2-yl)ethan-1-amine, (2-methoxy phenyl) methanamine, (4-fluorophenyl) methanamine) and solvents were purchased from Sigma Aldrich (India). Neat reactions were performed using sealed glass tubes. Thin layer chromatography was performed on pre-coated silica gel plates. One dimensional Nuclear Magnetic Resonance spectra were recorded in dimethyl sulfoxide DMSO-d_6 at 298 K (Bruker, ^{1}H NMR 400 MHz, ^{13}C NMR 100 MHz).NMR chemical shifts were referenced to the residual solvent signal of DMSO at δ 2.5 ppm for ^{1}H and at δ 40 ppm for ^{13}C. On the basis of their chemical shifts, signal intensities, multiplicity of resonances and H–H coupling constants, individual resonances were assigned. Single crystal XRD data were collected at Structural Crystallography Center, University of Florence, Sesto Fiorentino (Florence), Italy.

2.3. Experimental procedure for the synthesis of compounds (*1a-h*)

To 0.567 ml (1 eq) of 4-chloroquinaldine, R-NH_2 (1 eq) was slowly added at room temperature and the reaction mixture, in neat condition, was stirred at 180°C for 4 h. The completion of the reaction was monitored using thin layer chromatography. Once the reaction has been completed, the reaction mixture was cooled to room temperature and extracted with ethyl acetate. The combined organic layer was dried over anhydrous sodium sulfate and concentrated under reduced pressure. The reaction mixture was washed with hexane and ethyl acetate (10%) to get the pure product. The description of synthesis of the compounds **1a-h** and characterization are given in supporting information.

2.4. Crystallographic structure determination

X-ray diffraction measurements were performed on a Bruker X8 APEXII CCD diffractometer at room temperature. The data were processed using SAINT software [21]. The structures were solved by direct methods and refined by full-matrix least-squares techniques. Non-H atoms were refined with anisotropic displacement parameters. H atoms were inserted in calculated positions and refined with a riding model. The following computer programs and hardware were used: structure solution, SHELXS-97 and refinement, SHELXL-97 [22] and molecular diagrams, MERCURY [23].

2.5. Anticancer activity

The A549 cells (human lung carcinoma cell line) were cultured in DMEM medium supplemented with 10% fetal bovine serum (FBS) at 37 °C with 5% CO_2. The cell viability upon different compound treatments were evaluated in A549 cells by MTT (3-[4,5-methylthiazol-2-yl]-2,5-diphenyl-tetrazolium bromide) assay [24,25]. Briefly, A549 cells (10,000 cells/well) were seeded in a 96-well plate and incubated overnight. The next day, the culture medium was replaced with fresh DMEM (without FBS) and serial 10-fold dilutions of the test compounds were added. Negative control wells contained only the cells without any compound, and the blank wells contained only the culture medium without cells. The cells were placed back into the incubator for next 24 h. On the day of the assay, the cells were washed with phosphate buffer solution gently and 100 µl of it was added to each well, to this 5 µl of MTT reagent (10 mg/ml) was added per well and incubated for 4 h in dark. After completing the incubation, 100 µl of 100% DMSO was

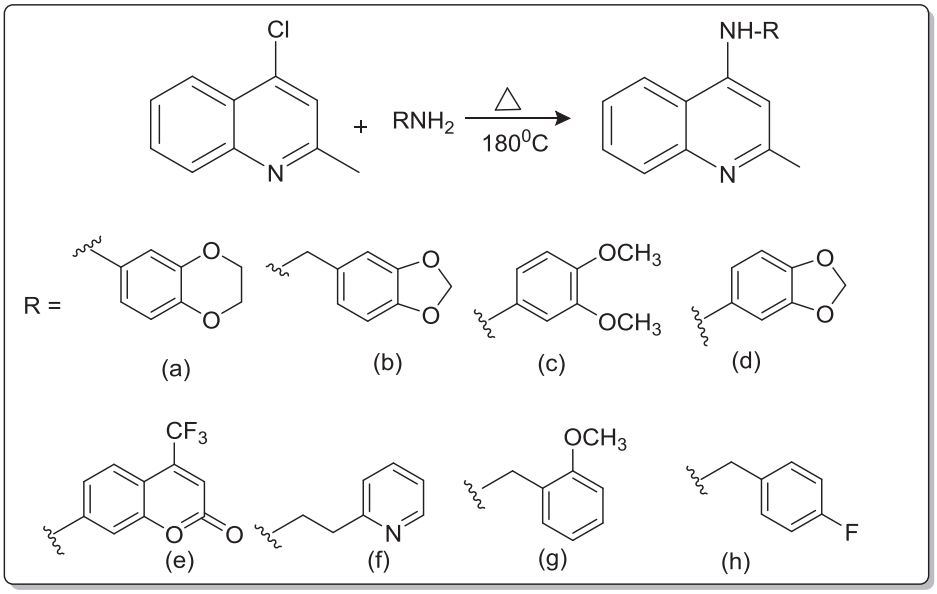

Scheme 1. Synthesis of 4-quinolineamines.

Table 1
Docking results of the designed compounds.

Compound	Docking score	Glide energy	Hydrogen bonded residues
Anilino quinoline	−6.356	−37.350	Ala162, Leu88
1a	−8.673	−45.661	Ala162
1b	−7.835	−41.115	Ala162, Leu88
1c	−8.472	−44.756	Ala162, Leu88
1d	−8.346	−42.103	Ala162, Lys111
1e	−8.535	−51.045	Ala162, Leu88, Lys111
1f	−7.624	−42.797	Ala162, Lys111
1g	−8.064	−43.236	Ala162, Lys111
1h	−7.749	−38.679	Ala162

added to each well and incubated in dark at room temperature for 1 h. The colour developed was measured as optical density (OD) at 570 nm. The percentage cell viability was calculated by ratio of the difference in the OD values obtained from wells carrying cells treated with compounds and the blank wells versus the difference in the OD values obtained in negative wells and the blank wells. To assess the compound's anticancer potency, the IC_{50} values (the concentration that inhibited cell viability to 50% of the control) were determined using Prism version 6 (GraphPad, San Diego, CA) by non-linear regression method.

3. Results and discussion

3.1. Computational approach

To design the compounds rationally for inhibiting the active site of PDK-1, the induced fit docking method was used in which both the protein and ligands are treated flexible so as to exactly predict the binding site of the amino quinoline analogs. The docking result of the anilino quinoline scaffold indicated that although it develops multiple interactions with Ala162, Leu88 it cannot interact with polar residues Thr222, Ser160 and other positively charged residues such as Lys111 that are located in the vicinity of the ring C and play important role in binding of GSK2334470, UCN01 and MP7 inhibitors. As shown in Fig. 3a, it can be observed that, the quinoline ring system sit well in the hinge region and the ring C in the solvent exposure region of the protein. By extending the methyl substituent, interactions with ser160 could be developed. The average distance from N2 position to Thr222 and Lys 111 (Fig. 3b) enables that, the linking of quinoline ring to ring C by addition of a methyl group at N2 position could make the molecule to adopt at the appropriate distance so as to develop interactions with Thr222 and Lys111. Also, addition of complementary negatively charged group from 3rd and 4th position of ring C could favorably develop interactions with the positively charge residues like Lys111 in its neighborhood.

To achieve this, we employed eight random substituents as shown in Scheme 1 to 2-methyl aminoquinoline with and without the methyl linker, positive and negatively charged groups at positions 3 and 4 of ring C. Another advantage is that, 2 and 4-substituted quinolines are easy to prepare as they are good nulcleophilic reaction sites. All the compounds except **1f** have negatively charged groups which can act as a hydrogen bond acceptor for the positively charged residues of PDK1 active site. From Fig. 3c, it is inferred that the addition of negatively charged groups at 3 and 4 could develop hydrogen bonding to Lys111, a positively charged aminoacid in the binding site. To evaluate this kind of designing approach and to predict their binding mode, IFD docking of the compounds with PDK1 was investigated. The docking results showed the improved docking scores and most of the compounds possess hydrogen bonds with Lys111 in addition to interactions with Ala162 when compared to parent anilino quinoline. The docking scores and glide energy were tabulated (Table 1). The synthesis of these eight compounds was then carried out.

3.2. Crystal structure

The single crystals of compounds (**1d, f-h**) were obtained by slow evaporation. The diffraction data were obtained to solve their three dimensional structures. The ortep plot of their thermal probability ellipsoids at 50% probability were given in Fig. 1. **1d** and **1h** were crystallized as two molecules in an asymmetric unit. As **(1d)** crystallized from methanol and toluene, the toluene contributed as half molecule in an asymmetric unit. The atomic positions of distorted five membered ring in **1a** was also refined using restraints. The quinoline system is found to be planar in all the structures. Among the four crystal structures (**1d, f-h**), the interplanar angle between quinoline ring system and the substituted amines deviates much in **1g** and **1h** (78.36° and 83.73° respectively) when compared to **1d** and **1f** (63.67° and 64.89° respectively). This planarity change was anticipated to make difference in binding in the PDK-1 active site. The details of crystal structure solution and refinement are given in Table 2.

Table 2
Crystal structure solution and refinement details.

Compound	1d	1f	1g	1h
Empirical formula	$4(C_{17}H_{14}N_2O_2)$, C_7H_8	$C_{17}H_{17}N_3$	$C_{18}H_{18}N_2O$	$C_{17}H_{15}FN_2$
Formula weight	1202.31	263.34	278.34	266.31
Temperature	293 K	293 K	293 K	293 K
Wavelength	0.71073 Å	1.54184 Å	0.71703 Å	
Crystal system	Triclinic	Monoclinic	Monoclinic	Triclinic
Space group	$P-1$	P 21/n	P 21/n	$P-1$
Unit cell dimensions	a = 10.0816(5) Å, b = 12.9268(6) Å, c = 12.9465(7) Å, α = 111.963(5)° β = 102.999(4)° γ = 92.068(4)°	a = 8.8917(3), b = 14.9336(7), c = 10.7455(5), α = 90° β = 97.306(4)° γ = 90°	a = 10.0610(8), b = 14.6561(11), c = 10.0750(8), α = 90° β = 99.107(7)° γ = 90°	a = 9.1057(8) Å, α = 111.963(5)° b = 9.7472(10) Å, β = 102.999(4)° c = 15.4797(12) Å, α = 97.615(7)° β = 99.954(7)° γ = 94.279(8)°
Volume	1511.13 (11) $Å^3$	1415.26(11) $Å^3$	1466.9(2) $Å^3$	1334.6(2) $Å^3$
Z	2	4	4	4
Density (calculated)	1.321 g/cm^3	1.236 g/cm^3	1.26 g/cm^3	1.325 g/cm^3
Absorption coefficient	0.087 mm^{-1}	0.582 mm^{-1}	0.079 mm^{-1}	0.089 mm^{-1}
F(0 0 0)	631	560	592	560
Theta range for data collection	4.10°–29.47°	5.08°–70.9°	4.64°–27.86°	4.1°–29.4°
Index ranges	$-13 \le h \le 13$, $-16 \le k \le 16$, $-17 \le l \le 17$	$-10 \le h \le 10$, $-18 \le k \le 17$, $-9 \le l \le 12$	$-13 \le h \le 7$, $-16 \le k \le 19$, $-11 \le l \le 12$	$-12 \le h \le 11$, $-12 \le k \le 12$, $-20 \le l \le 20$
Reflections collected	20056	10629	7097	6280
Independent reflections	7141 [R(int) = 0.0552]	2595 [R(int) = 0.051]	3246 [R(int) = 0.039]	6280 [Rint = 0.118]
Absorption correction	'multi-scan'	'multi-scan'	'multi-scan'	'multi-scan'
Max. and min. transmission	0.983 and 0.974	1.0 and 0.7099	0.992 and 1.0	0.963 and 1.0
Refinement method	Full-matrix least-squares on F^2	Full-matrix least-squares on F^2	Full-matrix least-squares on F^2	Full-matrix least-squares on F^2
Data/restraints/parameters	3947/3/447	2595/0/249	3246/0/250	6280/0/361
Goodness-of-fit on F^2	1.019	1.077	0.98	0.91
Final R indices	R_1 = 0.0641, wR_2 = 0.1292	R_1 = 0.0493, wR_2 = 0.1641	R_1 = 0.0566, wR_2 = 0.1559	R_1 = 0.0863, wR_2 = 0.2392
R indices (all data)	R_1 = 0.1326	R_1 = 0.0728	R_1 = 0.0905	R_1 = 0.2423
Largest diff. peak and hole	0.250 and −0.313 e.$Å^{-3}$	0.224 and −0.252 e.$Å^{-3}$	0.358 and −0.6803 e.$Å^{-3}$	0.464 and −0.254 e.$Å^{-3}$
CCDC number	1548778	1559837	1567175	1565972

Table 3
ADME properties predicted by Qikprop for compounds **1a-1 h.**

Compound	MW	Volume	QPlog Po/w	%Human oral absorption	PSA	Rule of five violation
1a	292.337	937.327	4.121	100	39.154	0
1b	292.337	938.618	3.958	100	40.712	0
1c	294.352	992.792	4.392	100	36.095	0
1d	278.31	873.89	3.739	100	40.622	0
1e	372.346	1073.548	4.455	100	61.73	0
1f	263.341	940.893	4.059	100	34.799	0
1g	278.353	966.366	4.377	100	29.279	0
1h	266.317	919.264	4.655	100	21.971	0

3.3. Antitumor activity by MTT assay

To analyze the efficiency of anticancer activity, the synthesized compounds were tested by MTT assay using lung adenocarcinoma A549, a non small cell lung cancer cell line. The expression pathways in A549 include PI3/AKT, MAPK, NF-kB etc in which PDK1 expression was reported as 14.7 TPM (transcripts per million) [26,27]. PDK1 downstreams the PI3K cell signaling pathways in cells and it was reported to be highly expressed in different lung cancer lines in addition to many breast cancer cells [26,3]. Pemetrexed, a lung cancer drug [28] was used as a positive control. The inhibitory efficiency of the compounds was assayed after 24h of incubation of the cells in drug-containing medium at a concentration range of 10^{-12} to 10^{-3} M. Significant inhibition of growth was defined as 60% or less of control cell growth. The obtained OD values for compounds **1a-h**, blank and control were given in detail as Table S1. The IC_{50} value determined from the plots for pemetrexed was found to be 1.15 μM. The activity of the test compounds was found to be in micromolar ranges whereas **1h** significantly inhibited the cancer cells with IC_{50} value of 0.96 μM which represents a better A549 cell line inhibitor than the Pemetrexed. Though, the inhibition mechanism of Pemetrexed is different, this MTT assay proved the better cytotoxicity of **1h** against A549 cell lines may be through inhibition of PDK1 or other mechanism which can be explained by further enzyme inhibition assays. When compared to all other compounds, **1b** and **1e** with IC_{50} values of 31.98 and 70.0 μM, respectively indicates futher tuning of their chemical structure will lead to a better inhibitor.

3.4. ADME prediction and binding mode analysis

The pharmacokinetic properties such as Absorption, Distribution, Metabolism and Excretion are more important in drug design [29]. The failure of anyone of these properties may lead to failure in druggability of the identified leads. The distribution of the drugs depends mainly on their binding with plasma protein [30]. The binding of all the test compounds with human serum albumin were confirmed by multi spectroscopic methods with binding constants in 10^4 to 10^5 ranges (our previous reports). The ADME properties were also predicted using Qikprop in Schrodinger which indicates that all the compounds possess full human oral absorption and none of the Lipinski rules of 5 is violated. The octanol-water coefficients which denote the hydrophobicity of the compounds was also found to be well within the normal range of other standard drugs (Table 3).

In order to analyze the binding mode of the compounds, the three dimensional coordinates obtained from the crystal structure obtained for **1d, 1f-1h** were docked with PDK-1 and the obtained complex

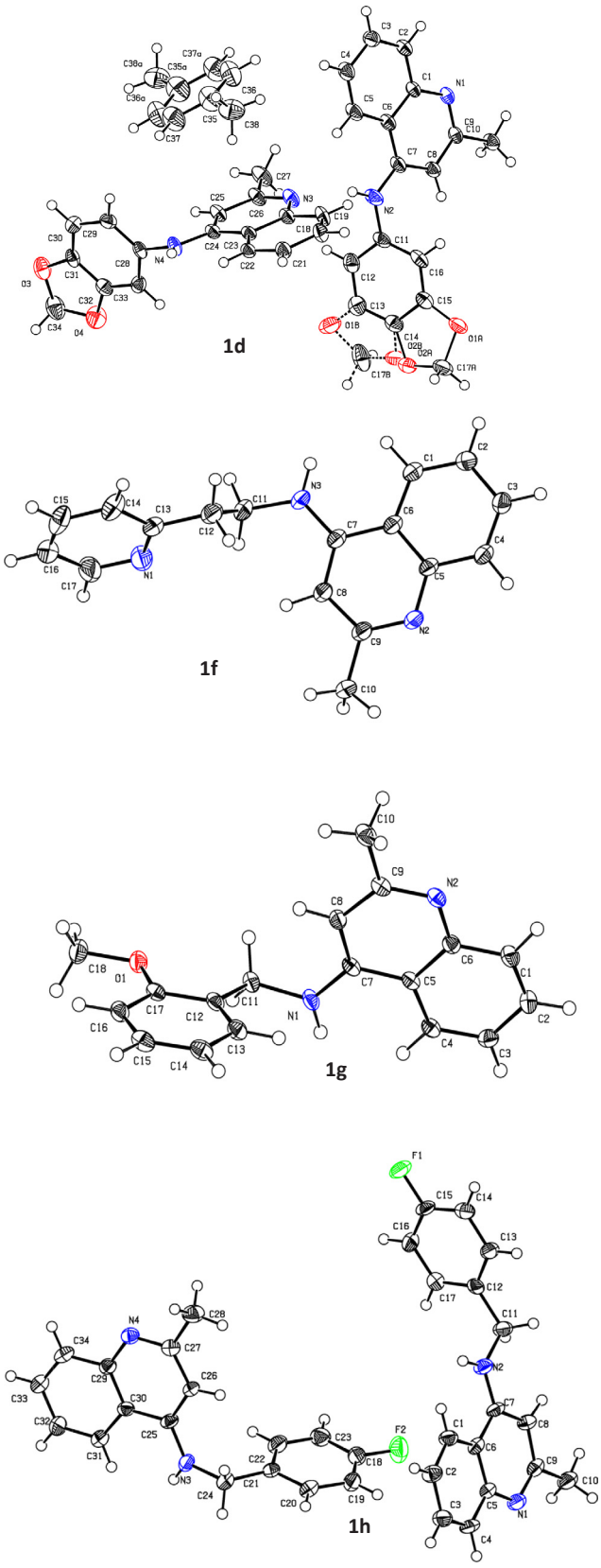

Fig. 4. ORTEP plots showing thermal ellipsoids at 50% probability level.

structures were superimposed with complex crystal structure with PS653 (PDB ID: 5LVL) and the superposition revealed that the quinoline scaffold exactly sit in the same position as PS653 and the substituents at N_2 made the difference in interacting with the protein. Also it can be

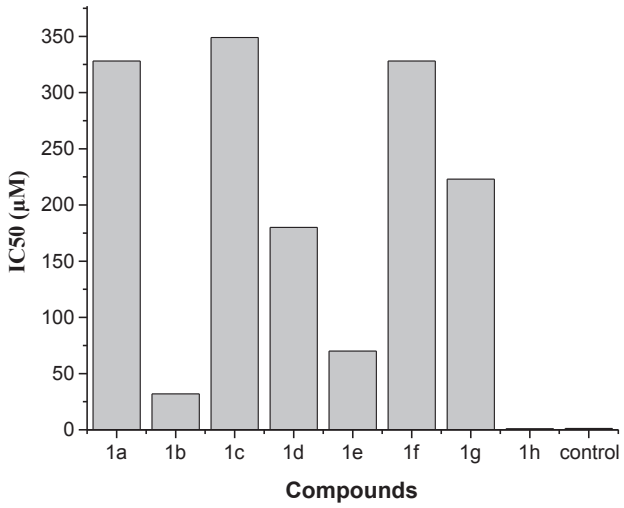

Fig. 5. IC_{50} values determined from MTT assay.

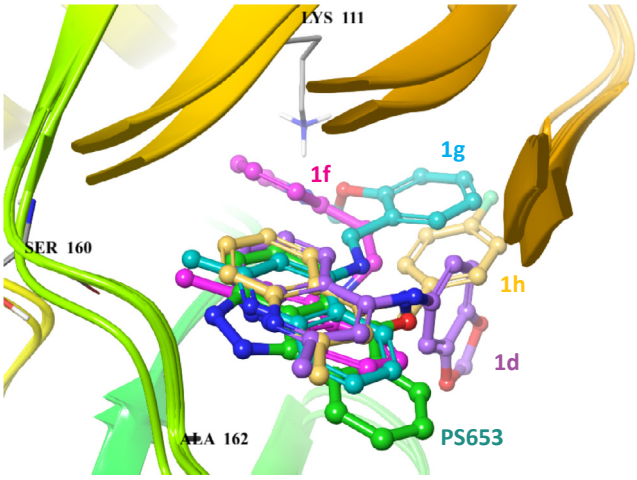

Fig. 6. Superposition of the docked complexes of **1d**, **1f**, **1g** and **1h** with co-crystallized complex of PS653 and PDK1.

observed from Fig. 4, the addition of any positively charged group instead of methyl group in quinoline ring system might develop hydrogen bond with Ser160. This type of hydrogen bonding with Ser160 was observed in almost all the cocrystallized ligands with PDK-1 in PDB. The angular difference between the quinoline scaffold and the amine substituents among these four compounds were found to influence their docking scores and activity (see Figs. 5 and 6).

4. Conclusion

Quinoline scaffold is identified to bind in the hydrophobic space of the active site in PDK1. Eight new derivatives were designed based on induced fit docking results of anilino quinoline with PDK1. The three dimensional crystal structures of amino substituted quinoline analogs were determined and the coordinates obtained were used for IFD and the comparison of their binding mode with PS653 indicates that further tuning of **1b**, **1e** and **1h** will provide a better lead. The screening of compounds against A549 cell lines identified **1h** with IC_{50} value of 0.96 μM which is lesser when compared to Pemetrexed, a marketed lung cancer drug. It is proposed that the compound **1h** with further modification and by PDK1 enzyme inhibition assay will give us the potent inhibitor of PDK and it is planned for the future work.

Acknowledgements

KNV thanks DST, Govt. of India for funding through WOS-A scheme. The authors also acknowledge the DST-FIST NMR facility, Gandhigram Rural Institute-Deemed to be University. KNV also acknowledges the computational facility and Schrodinger access offered by Prof. D. Velmurugan, BSR Faculty, Center for crystallography and Biophysics, University of Madras, Chennai.

Appendix A. Supplementary material

Supplementary data associated with this article can be found, in the online version, at https://doi.org/10.1016/j.bioorg.2018.08.007.

References

[1] S. Sansook, C.A. Ocasio, I.J. Day, G.J. Tizzard, S.J. Coles, O. Fedorov, J.M. Bennett, J.M. Elkins, J. Spencer, Synthesis of kinase inhibitors containing a pentafluorosulfanyl moiety, Org. Biomol. Chem. 15 (2017) 8655–8660, https://doi.org/10.1039/c7ob02289a.

[2] L. Di Blasio, P.A. Gagliardi, A. Puliafito, L. Primo, Serine/threonine kinase 3-phosphoinositide-dependent protein kinase-1 (PDK1) as a key regulator of cell migration and cancer dissemination, Cancers (Basel) 9 (2017) 25–41, https://doi.org/10.3390/cancers9030025.

[3] C. Fyffe, M. Falasca, 3-Phosphoinositide-dependent protein kinase-1 as an emerging target in the management of breast cancer, Cancer Manag. Res. 5 (2013) 271–280, https://doi.org/10.2147/CMAR.S35026.

[4] P. Armando Gagliardi, L. di Blasio, F. Orso, G. Seano, R. Sessa, D. Taverna, F. Bussolino, L. Primo, 3-Phosphoinositide-dependent kinase 1 controls breast tumor growth in a kinase-dependent but akt-independent manner, 719-IN19, Neoplasia 14 (2012) 719–731, https://doi.org/10.1593/neo.12856.

[5] S.W.S. Hann, Q. Tang, F. Zheng, S. Zhao, J. Chen, Z.Y. Wang, Repression of phosphoinositide-dependent protein kinase 1 expression by ciglitazone via Egr-1 represents a new approach for inhibition of lung cancer cell growth, Mol. Cancer. 13 (2014) 1–13, https://doi.org/10.1186/1476-4598-13-149.

[6] R. Arsenic, Immunohistochemical analysis of PDK1 expression in breast cancer, Diagn. Pathol. 9 (2014) 82–84, https://doi.org/10.1186/1746-1596-9-82.

[7] J. Du, M. Yang, S. Chen, D. Li, Z. Chang, Z. Dong, PDK1 promotes tumor growth and metastasis in a spontaneous breast cancer model, Oncogene 35 (2016) 3314–3323, https://doi.org/10.1038/onc.2015.393.

[8] T. Tamgüney, C. Zhang, D. Fiedler, K. Shokat, D. Stokoe, Analysis of 3-phosphoinositide-dependent kinase-1 signaling and function in ES cells, Exp. Cell Res. 314 (2008) 2299–2312, https://doi.org/10.1016/j.yexcr.2008.04.006.

[9] M. Brzozowski, N.J. O'Brien, D.J.D. Wilson, B.M. Abbott, Synthesis of substituted 4-(1H-indol-6-yl)-1H-indazoles as potential PDK1 inhibitors, Tetrahedron 70 (2014) 318–326, https://doi.org/10.1016/j.tet.2013.11.054.

[10] J.R. Medina, C.J. Becker, C.W. Blackledge, C. Duquenne, Y. Feng, S.W. Grant, D. Heerding, W.H. Li, W.H. Miller, S.P. Romeril, D. Scherzer, A. Shu, M.A. Bobko, A.R. Chadderton, M. Dumble, C.M. Gardiner, S. Gilbert, Q. Liu, S.K. Rabindran, V. Sudakin, H. Xiang, P.G. Brady, N. Campobasso, P. Ward, J.M. Axten, Structure-based design of potent and selective 3-phosphoinositide-dependent kinase-1 (PDK1) inhibitors, J. Med. Chem. 54 (2011) 1871–1895, https://doi.org/10.1021/jm101527u.

[11] E.V. Bobkova, M.J. Weber, Z. Xu, Y.-L. Zhang, J. Jung, P. Blume-Jensen, A. Northrup, P. Kunapuli, J.N. Andersen, I. Kariv, Discovery of PDK1 kinase inhibitors with a novel mechanism of action by ultra-high throughput screening, J. Biol. Chem. 285 (2010) 18838–18846, https://doi.org/10.1074/jbc.M109.089946.

[12] A. Gopalsamy, M. Shi, D.H. Boschelli, R. Williamson, A. Olland, Y. Hu, G. Krishnamurthy, X. Han, K. Arndt, B. Guo, Discovery of dibenzo[c, f][2,7]naphthyridines as potent and selective 3-phosphoinositide-dependent kinase-1 inhibitors, J. Med. Chem. 50 (2007) 5547–5549, https://doi.org/10.1021/jm070851i.

[13] T. Nittoli, R.G. Dushin, C. Ingalls, K. Cheung, M.B. Floyd, H. Fraser, A. Olland, Y. Hu, G. Grosu, X. Han, K. Arndt, B. Guo, A. Wissner, The identification of 8,9-dimethoxy-5-(2-aminoalkoxy-pyridin-3-yl)-benzo[c][2,7]naphthyridin-4-ylamines as potent inhibitors of 3-phosphoinositide-dependent kinase-1 (PDK-1), Eur. J. Med. Chem. 45 (2010) 1379–1386, https://doi.org/10.1016/j.ejmech.2009.12.036.

[14] S. Sestito, G. Nesi, S. Daniele, A. Martelli, M. Digiacomo, A. Borghini, D. Pietra, V. Calderone, A. Lapucci, M. Falasca, P. Parrella, A. Notarangelo, M.C. Breschi, M. Macchia, C. Martini, S. Rapposelli, Design and synthesis of 2-oxindole based multi-targeted inhibitors of PDK1/Akt signaling pathway for the treatment of glioblastoma multiforme, Eur. J. Med. Chem. 105 (2015) 274–288, https://doi.org/10.1016/j.ejmech.2015.10.020.

[15] N.J. O'Brien, M. Brzozowski, D.J.D. Wilson, L.W. Deady, B.M. Abbott, Synthesis and biological evaluation of substituted 2-anilino-7H-pyrrolopyrimidines as PDK1 inhibitors, Tetrahedron 70 (2014) 4947–4956, https://doi.org/10.1016/j.tet.2014.05.033.

[16] J.O. Schulze, G. Saladino, K. Busschots, S. Neimanis, E. Süß, D. Odadzic, S. Zeuzem, V. Hindie, A.K. Herbrand, M.N. Lisa, P.M. Alzari, F.L. Gervasio, R.M. Biondi, Bidirectional allosteric communication between the ATP-binding site and the regulatory PIF pocket in PDK1 protein kinase, Cell Chem. Biol. 23 (2016) 1193–1205, https://doi.org/10.1016/j.chembiol.2016.06.017.

[17] T.J. Rettenmaier, J.D. Sadowsky, N.D. Thomsen, S.C. Chen, A.K. Doak, M.R. Arkin, J.A. Wells, A small-molecule mimic of a peptide docking motif inhibits the protein kinase PDK1, Proc. Natl. Acad. Sci. 111 (2014) 18590–18595, https://doi.org/10.1073/pnas.1415365112.

[18] N.J. O'Brien, M. Brzozowski, D.J.D. Wilson, L.W. Deady, B.M. Abbott, Synthesis and biological evaluation of substituted 3-anilino-quinolin-2(1H)-ones as PDK1 inhibitors, Bioorg. Med. Chem. 22 (2014) 3781–3790, https://doi.org/10.1016/j.bmc.2014.04.037.

[19] G. Madhavi Sastry, M. Adzhigirey, T. Day, R. Annabhimoju, W. Sherman, Protein and ligand preparation: Parameters, protocols, and influence on virtual screening enrichments, J. Comput. Aided. Mol. Des. 27 (2013) 221–234, https://doi.org/10.1007/s10822-013-9644-8.

[20] D. Shivakumar, J. Williams, Y. Wu, W. Damm, J. Shelley, W. Sherman, Prediction of absolute solvation free energies using molecular dynamics free energy perturbation and the OPLS force field, J. Chem. Theory Comput. 6 (2010) 1509–1519, https://doi.org/10.1021/ct900587b.

[21] Bruker, APEX2 and SAINT Programs for Data Reduction, Apex II. (2009) Bruker AXS Inc., Madison, Wisconsin, USA.

[22] G.M. Sheldrick, Crystal structure refinement with SHELXL, Acta Crystallogr. Sect. C Struct. Chem. 71 (2015) 3–8, https://doi.org/10.1107/S2053229614024218.

[23] C.F. Macrae, P.R. Edgington, P. McCabe, E. Pidcock, G.P. Shields, R. Taylor, M. Towler, J. van De Streek, Mercury: visualization and analysis of crystal structures, J. Appl. Crystallogr. 39 (2006) 453–457, https://doi.org/10.1107/s002188980600731x.

[24] S.R. D'Mello, K. Borodezt, S.P. Soltoff, Insulin-like growth factor and potassium depolarization maintain neuronal survival by distinct pathways: possible involvement of PI 3-kinase in IGF-1 signaling, J. Neurosci. 17 (1997) 1548–1560.

[25] J. Wang, J. Li, A. Lu, K. Zhang, B. Li, Anticancer effect of salidroside on A549 lung cancer cells through inhibition of oxidative stress and phospho-p38 expression, Oncol. Lett. (2014) 1159–1164, https://doi.org/10.3892/ol.2014.1863.

[26] N. Khan, N. Hadi, F. Afaq, D.N. Syed, M.H. Kweon, H. Mukhtar, Pomegranate fruit extract inhibits prosurvival pathways in human A549 lung carcinoma cells and tumor growth in athymic nude mice, Carcinogenesis. 28 (2007) 163–173, https://doi.org/10.1093/carcin/bgl145.

[27] L. Korrodi-Gregório, V. Soto-Cerrato, R. Vitorino, M. Fardilha, R. Pérez-Tomás, From proteomic analysis to potential therapeutic targets: Functional profile of two lung cancer cell lines, A549 and SW900, widely studied in pre-clinical research, PLoS One. 11 (2016) 1–27, https://doi.org/10.1371/journal.pone.0165973.

[28] M.H. Cohen, J.R. Johnson, Y.C. Wang, R. Sridhara, R. Pazdur, FDA drug approval summary: pemetrexed for injection (Alimta) for the treatment of non-small cell lung cancer, Oncologist. 10 (2005) 363–368, https://doi.org/10.1634/theoncologist.10-6-363.

[29] C.A. Lipinski, F. Lombardo, B.W. Dominy, P.J. Feeney, Experimental and computational approaches to estimate solubility and permeability in drug discovery and develop ment settings, Adv. Drug Deliv. Rev. 23 (1997) 3–25, https://doi.org/10.1016/S0169-409X(00)00129-0.

[30] X. Liu, M. Wright, C.E.C.A. Hop, Rational use of plasma protein and tissue binding data in drug design, J. Med. Chem. 57 (2014) 8238–8248, https://doi.org/10.1021/jm5007935.

[31] L. Schrödinger, Maestro 8.5 user manual, Schrödinger Press, 2008.